

Chapter 1

Concepts of Material Fatigue

1.1. Introduction

1.1.1. Reminders on the strength of materials

1.1.1.1. Hooke's law

We accept that the strain at a point of a mechanical part is proportional to the elastic force acting on this point. This law assumes that the strains remain very small (elastic phase of the material). It enables us to establish a linear relationship between the forces and the deformation or between the stresses and the strains. In particular, if we consider the normal stress and the shear stress, we can write successively

$$\sigma = E \varepsilon_n \quad [1.1]$$

$$\tau = G \varepsilon_t \quad [1.2]$$

where

E = Young's modulus or elastic modulus

G = shear modulus or Coulomb's modulus

2 Fatigue Damage

ε_n = tensile strain parallel to the axis of the part ($= \frac{\Delta \ell}{\ell}$) if ℓ is the initial length of the object and $\Delta \ell$ is its extension.

ε_t = relative strain in the plane of the cross-section

The following table gives several values of the Young's modulus E:

Material	Young's modulus E (Pa)
Steel	2 to 2.2 10^{11}
Brass	1 to 1.2 10^{11}
Copper	1.1 10^{11}
Zinc	9.5 10^{10}
Lead	5 10^9
Wood	7 to 11 10^9

Table 1.1. Some values of Young's modulus

NOTE.— Hooke's law is only an approximation of the real relationship between stress and strain, even for small stresses [FEL 59]. If Hooke's law is perfectly respected, the stress strain process would thus be, below the elastic limit, thermodynamically reversible, with complete restitution of the energy stored in the material. Experience shows that this is not the case and that, even at very low levels of stress, a hysteresis exists. The process is never perfectly reversible.

1.1.1.2. Stress-strain curve

Engineering stress-strain curve

Let us consider the curve obtained by carrying out a tensile test on a cylindrical sample of length ℓ , made of mild steel for example, and by tracing the traction force F according to the extension $\Delta \ell$ that the sample experiences or, which amounts to the same thing, the normal stress $\sigma = \frac{F}{S}$ according to the relative expansion

$\epsilon = \frac{\Delta \ell}{\ell}$ (strain). The test is carried out by making force F grow progressively, starting from zero.

The *stress strain curve* thus obtained, traced in the axes (σ, ϵ) , has an identical shape since the changing of the variable corresponds to a proportional transformation (S cross-section, ℓ useful length of the bar). This dimensionless diagram is characteristic of the material here, and not of the sample considered (Figure 1.1).

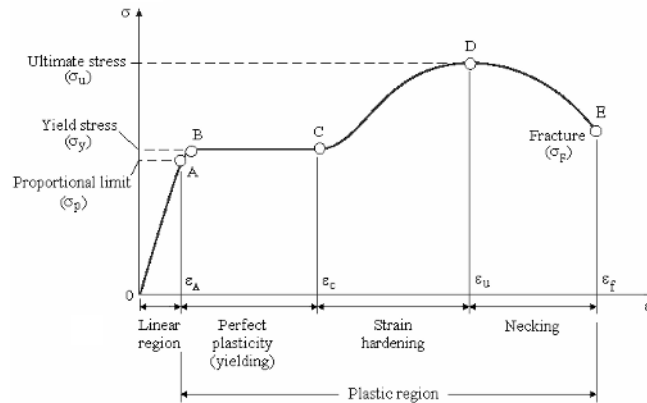


Figure 1.1. Stress–strain diagram of a ductile material.

σ_u = ultimate stress, σ_y = yield stress, σ_p = proportional limit,
 σ_F = fracture stress OA = linear region, AE = plastic region

This curve can be broken down into four arcs. Arc OA corresponds to the *elastic region* where the strain is reversible; the elongation there is proportional to the force (Hooke’s law):

$$\Delta \ell = F \frac{\ell}{E S_0} \tag{1.3}$$

(E = Young’s modulus, S_0 = initial cross-section of the sample of length ℓ).

This relation can also be written

4 Fatigue Damage

$$\sigma = E \frac{\Delta \ell}{\ell} \quad [1.4]$$

($\sigma = \frac{F}{S}$). In reality, the expansions $\Delta \ell$ of this zone are very small and the above curve is very badly proportioned.

There are several definitions of the elastic limit, chosen according to the case for an elongation of 0.01 %, 0.1 % or 0.2 %, the latter value being the most frequently used.

We call the *proportional limit* σ_p the maximum stress up to which the material does not show residual strain after unloading [FEO 69].

The BC zone, called the *yielding region*, corresponds to a significant stretching of the sample for an almost constant traction force. This stage has a variable length according to the materials; it can possibly be unnoticeable on some recordings. The strain is permanent and homogeneous.

The yield stress σ_y is the stress beyond which the strain increases without a notable increase in the load (point B). We call the *ultimate tensile strength* (UTS) σ_u the ratio between the maximum force F_{\max} that a sample can bear and the initial area S_0 of the cross-section of the sample before testing (Figure 1.1):

$$\sigma_u = \frac{F_{\max}}{S_0} \quad [1.5]$$

The CD zone, *strain hardening region*, represents an elongation of the sample with the force which is produced much more slowly than in the elastic zone. Work hardening corresponds to a plastic strain of the metal at a temperature lower than the recrystallization temperature (which makes it possible to replace the strained, work-hardened structure with a new structure with reformed grains).

If, after having increased the force F from 0 to F_m such that the point m belongs to arc CD, the load is decreased, we notice that the point shows the straight segment mn going from m and parallel to OA (Figure 1.2). For a zero load, there remains a residual elongation. This is called *plastic extension*. The strain is permanent.

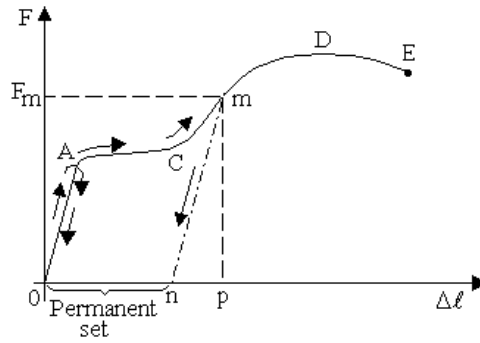


Figure 1.2. *Plastic expansion*

Let us recall that as long as point $(F, \Delta \ell)$ remains on OA , it describes this segment in the opposite direction if the load is taken back to zero. OA is a perfectly elastic zone, not leading to a residual elongation.

If, from n , the sample is loaded again, the new diagram is made up of arcs nm , mDE (Figure 1.3). We note that the rectilinear segment (elastic zone) of the work-hardened bar is longer than OA . A stretched material can thus bear greater loads without residual strain.

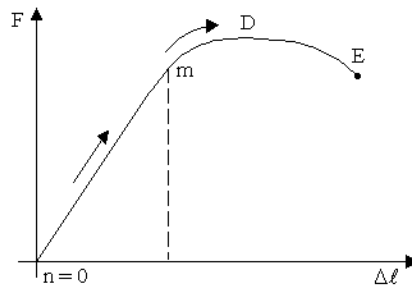


Figure 1.3. *New diagram after plastic strain*

The mechanical properties of a work-hardened metal are modified a lot: the elastic limit, the breaking load and the hardness are greatly increased, the expansion to fracture, the resistance and the necking are generally reduced.

It is in this zone that the neck is formed, the part of the sample where the cross-section reduces as quickly when the load increases, thus setting the future fracture

area (necking phenomenon). The force F passes through a maximum (at D) when the relative reduction of the area S in this domain becomes equal to the relative increase of the stress.

Between D and E, the extension of the bar is produced with a reduction of the force F (the average stress in the area of the neck continues to grow however). Necking is when the specimen's cross-section starts to stretch significantly. The size of the neck varies with the nature of the material.

When the metal begins to *neck*, as the cross-sectional area of the specimen decreases due to plastic flow, it causes a reversal of the engineering stress–strain curve; this is because the *engineering stress* is calculated assuming the original cross-sectional area (S_0) before necking.

DE is the *necking region* [FEO 69]. At E, the sample fractures. The *fracture strength* σ_F is the ratio between the load to fracture F_F and the cross-sectional area S_0 :

$$\sigma_F = \frac{F_F}{S_0} \quad [1.6]$$

These definitions assume that the cross-section and the length of the sample do not vary much during the application of the load. In most practical applications, this hypothesis leads to results that are precise enough. The stress–strain curve traced with these definitions is called the *engineering stress–strain curve* (Figure 1.4).

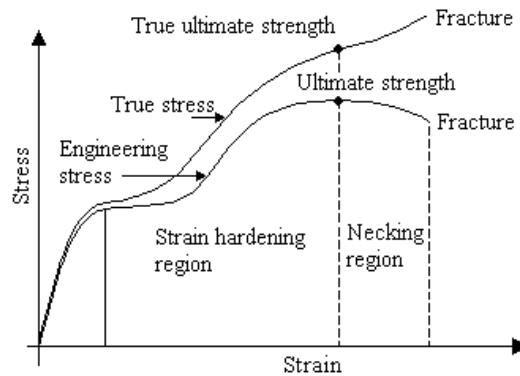


Figure 1.4. Stress–strain diagram – ultimate tensile strength and true ultimate strength

True stress–strain curve

In reality, beyond the elastic limit, the dimensions of the sample change when the load is applied. It is thus more exact to define the stresses by dividing the applied force by the real cross-section of the sample.

We call the *true tensile ultimate strength* σ_{ut} the ratio between the maximum force F_{max} that a sample can bear and the area S_{mt} of the true cross-section of the sample when the force is equal to F_{max} :

$$\sigma_{ut} = \frac{F_{max}}{S_{mt}} \quad [1.7]$$

The *true fracture strength* σ_{Ft} is the load at fracture F_F divided by the true cross-sectional area S_{Ft} of the sample [LIU 69].

$$\sigma_{Ft} = \frac{F_F}{S_{Ft}} \quad [1.8]$$

The stress–strain curve obtained in these conditions is called the *true stress–strain curve* (Figure 1.4).

Like the ultimate tensile strength, the true fracture strength can help an engineer to predict the behavior of the material, but is not itself a practical strength limit.

If S_0 is the initial cross-sectional area of the piece and S_t is the area of the section after work hardening, we call the *work-hardening rate* the ratio $\frac{S_0 - S_t}{S_t} 100$.

Finally, we call the *strain at break* δ (%) the average residual strain which takes place at the time of fracture, linked to a determined length of the sample. If d is the diameter of the bar before testing, the standard length chosen is $5d = \ell_0$

$$\delta(\%) = \frac{\Delta \ell_0}{\ell_0} 100 \quad [1.9]$$

A material is more plastic the larger the value of δ . δ characterizes the ability of the material to show large residual strains without fracture.

The materials which, on the other hand, split without going through significant residual strains are called *brittle*.

Fragility is thus the opposite of plasticity. These materials have stress strain curves without a stretching stage and without a work-hardening zone. Their resistance to tension coincides in practice with their stretching limit (Figure 1.5).

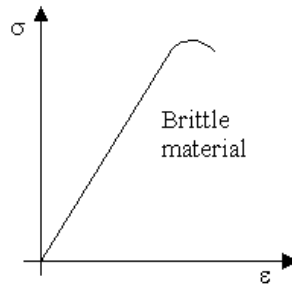


Figure 1.5. *Diagram for a brittle material*

It should be noted that the values defined here for a tension test can also be defined in compression. Furthermore, for the same material, we see differences in the numerical values of these parameters according to the nature of the stress.

The materials can naturally also break under the effects of compression. Plastic materials above all have a curve comparable to that in tension, with an elastic zone, stretching stage, work-hardening zone, etc. Beyond this, the curve, instead of decreasing, increases rapidly, the cross-section of the compressed material then increases after a barrel-like distortion in the sample.

Let us finally recall that we call *hardness* the property of the material to resist mechanical penetration of other bodies [FEO 69] (Brinell, Rockwell, hardness, etc.).

We will not study variations of the properties according to the temperature here.

NOTE.—

All the observations above correspond to the case where the force F is applied very slowly. Materials have a different behavior under dynamic loads. Two criteria can be retained to evaluate this type of load:

– we can consider that the load varies quickly if it transmits significant speeds to particles of the body under strain, so that the total kinetic energy of the masses in

movement make up a significant part of the total work of the exterior forces; this first criterion is the one used during the analysis of the oscillations of elastic bodies;

– we can link the speed of variation of the load to the speed of evolution of the plastic strains, the preferred process during the study of the mechanical properties of the materials when there is a quick strain.

1.1.1.3. Poisson's ratio

A bar subjected to tension forces is subject to two types of strain:

– an extension $\Delta\ell$ or $\varepsilon_x = \frac{\Delta\ell}{\ell}$ along its longitudinal axis;

– a transversal reduction ε_y . Experience shows that $\varepsilon_y = -\nu \varepsilon_x$, where ν is a constant of the material called *Poisson's ratio*.

For metals, ν varies from 0.25 to 0.35. It is close to 0.3 for steels and aluminum alloys.

1.1.2. Fatigue

Fatigue phenomena, with formation and growth of cracks in machine elements subjected to repeated loads below ultimate strength, was discovered during the 19th century with the arrival of machines and freight vehicles functioning under dynamic loads larger than those encountered before [NEL 78].

According to H.F. Moore and J.B. Koppers [MOO 27], the first work published on failure by fatigue was by W. Albert, a German mining engineer. In 1829 he carried out repeated loading tests on welded chains of mine winches. S.P. Poncelet was perhaps the first to use the term *fatigue* in 1839 [TIM 53].

The most important problems of failure by fatigue were found around 1850 during the development of the European railroad (axes of car wheels). An initial explanation was that metal crystallizes under the action of the repeated loads, until failure. The source of this idea is the coarsely crystalline appearance of many surfaces of parts broken by fatigue. This theory was disparaged by W.J. Rankine [RAN 43] in 1843. The first tests were carried out by Wöhler between 1852 and 1869 [WÖH 60].

The dimensioning of a structure to fatigue is more difficult than with static loads [ROO 69] because ruptures by fatigue depend on localized stresses. Since the fatigue stresses are in general too low to produce a local plastic deformation and the redistribution associated with the stresses, it is necessary to carry out a detailed

analysis which takes into account both the total model of the stresses and the strong localized stresses due to the concentrations.

On the other hand, analysis of static stresses only requires the definition of the total stress field, the high localized stresses being redistributed by local deformation. Three fundamental steps are necessary:

- definition of the loads;
- detailed analysis of the stresses; and
- consideration of the statistical variability of the loads and the properties of materials.

Fatigue damage strongly depends on the oscillatory components of the load, its static component and the order of application of the loads.

Fatigue can be approached in several ways and, in particular, by:

- the study of Wöhler's curves (stress versus number of cycles, or S-N, curves);
- the study of cyclic work hardening (low-cycle fatigue); and
- the study of the crack propagation rate (fracture mechanics).

The first of these approaches is the most used. We will present some aspects of them in this chapter.

1.2. Types of dynamic loads (or stresses)

The load applied to equipment can vary in different ways:

- periodic or *cyclic*;
- random; or
- quickly between two stationary states (*transitory*).

It can also be zero average, any average, constant or not.

1.2.1. *Cyclic stress*

In the simplest case, the load applied varies in a sinusoidal manner between σ_{\max} and σ_{\min} around the rest position (zero mean).

Consider a stress $\sigma(t)$ varying periodically in time; $\sigma(t)$ values over a period (the smallest part of the function periodically repeating) are called “cycle of stress”. The most common cycle is the sinusoidal cycle.

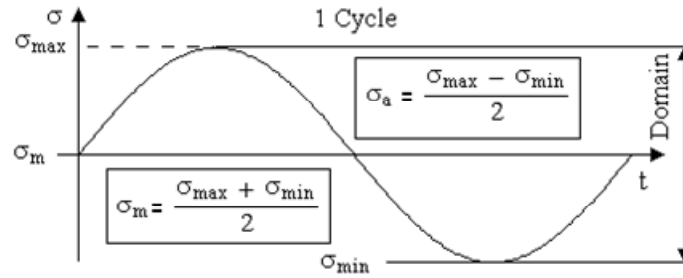


Figure 1.6. *Non-zero mean sinusoidal cycle of stress*

We refer to the largest algebraic value of the stress during a cycle as *maximum stress* σ_{\max} and the smallest algebraic value (the traction stress being positive) as the *minimum stress* σ_{\min} .

The *mean stress* σ_m is the permanent (or static) stress on which the cyclic stress is superimposed.

σ_a is the amplitude of the oscillatory stress $\sigma_a = \sigma_{\max} - \sigma_m$.

We define the *cycle coefficient* or *stress variation rate* (or “*stress ratio*”) as:

$$R = \frac{\sigma_{\min}}{\sigma_{\max}} \quad [1.10]$$

We also define another parameter A:

$$A = \frac{\sigma_a}{\sigma_m} \quad [1.11]$$

which relates the alternating stress amplitude to the mean stress. A and R are linked by equation [1.12]:

$$R = \frac{1-A}{1+A} \quad \text{or} \quad A = \frac{1-R}{1+R} \quad [1.12]$$

We refer to the difference

$$\sigma_d = \sigma_{\max} - \sigma_{\min} = 2 \sigma_a \quad [1.13]$$

as the *range of stress*. σ_a is called the *purely alternating stress* when it varies between equal positive and negative values.

1.2.2. Alternating stress

An *alternating stress* evolves between a positive maximum and a negative minimum where absolute values are different.

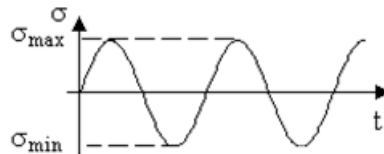


Figure 1.7. *Alternating stress (completely reversed stressing)*

In the case of a zero mean stress ($\sigma_m = 0$), we have $R = -1$ and the cycle is said to be *symmetric* or *alternating symmetric* [BRA 81], [CAZ 69], [RAB 80], [RIC 65b].

The cyclic load can also be superimposed on a constant static load σ_m . If σ_a is the cyclic load amplitude:

$$\sigma_{\max} = \sigma_m + \sigma_a$$

$$\sigma_{\min} = \sigma_m - \sigma_a$$

When σ_{\min} or σ_{\max} is zero, the cycle is said to be *pulsating* [FEO 69].

Two cycles are *similar* if they have the same R coefficient.

When R is ordinary, we can consider that such a cycle is the superimposition of:

– a constant stress σ_m

– a symmetric cyclic stress of amplitude σ_a . We have:

$$\sigma_m = \frac{\sigma_{\max} + \sigma_{\min}}{2} = \frac{\sigma_{\max}}{2} (1 + R) \quad [1.14]$$

$$\sigma_a = \frac{\sigma_{\max} - \sigma_{\min}}{2} = \frac{\sigma_{\max}}{2} (1 - R) \quad [1.15]$$

It is considered that the endurance of a component does not depend on the law of variation in the interval $(\sigma_{\max}, \sigma_{\min})$. We also ignore the influence of the frequency of the cycle [RIC 65b].

1.2.3. Repeated stress

When the stress varies between 0 and $\sigma_{\max} > 0$, between 0 and $\sigma_{\min} < 0$, i.e. when $R = 0$, we say that the load is *repeated* ($\sigma_m = \sigma_a$).

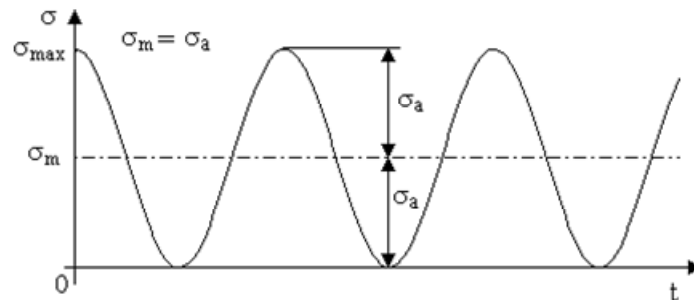


Figure 1.8. Repeated stress (zero-to-tension stressing)

1.2.4. Combined steady and cyclic stress

The stress is said to be combined steady and cyclic or fluctuating when $0 < R < 1$ ($\sigma_m > \sigma_a$), i.e. when σ_{\max} and σ_{\min} are similar.

1.2.5. Skewed alternating stress

In this case, $-1 < R < 0$ (with $0 < \sigma_m < \sigma_a$).

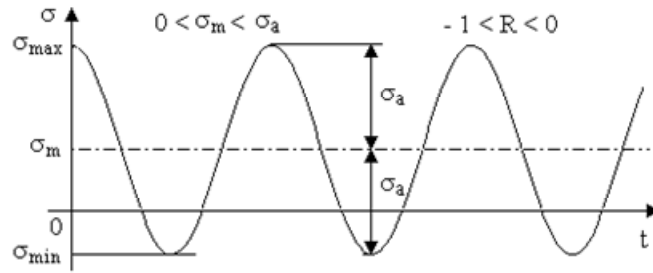


Figure 1.9. Skewed alternating stress

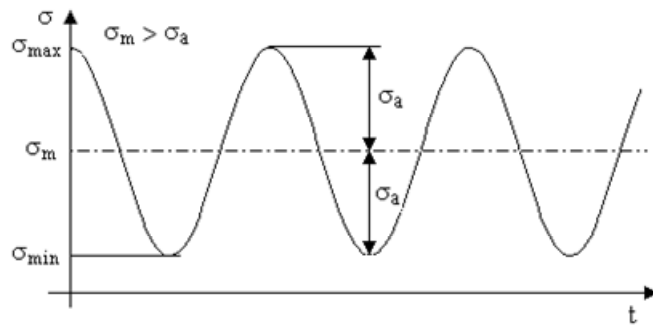


Figure 1.10. Combined steady and cyclic stress ($0 < R < 1$)

These cyclic loads can be encountered e.g. in rotating machines.

1.2.6. Random and transitory stresses

In many cases, we cannot consider vibrations as sinusoidal. For example, vibrations from an aircraft's floor or on missile devices are *random* vibrations with randomly variable amplitude in time. Energy is distributed in a wide frequency interval, instead of being centered on a given frequency (Volume 1, Chapter 1 and Volume 3).

Other phenomena such as shocks measured on an aircraft's landing gear, the starting or stopping of rotating machines, missile and launcher staging, etc. are all transitory, either centered on a given frequency or not.

All these loads lead to effects of fatigue that are much harder to evaluate experimentally, especially in a projected manner. In the following sections, we will show how we can estimate them.

1.3. Damage arising from fatigue

We define the modification of the characteristics of a material, primarily due to the formation of cracks and resulting from the repeated application of stress cycles, as *fatigue damage*. This change can lead to a failure.

We will not consider here the mechanisms of nucleation and growth of the cracks. We will simply state that fatigue starts with a plastic deformation, initially highly localized around certain macroscopic defects (inclusions, cracks of manufacture, etc.), under total stresses which can be lower than the yield stress of the material. The effect is extremely weak and negligible for only one cycle. If the stress is repeated, each cycle creates a new localized plasticity. After a number of variable cycles, depending on the level of the applied stress, ultra-microscopic cracks can be formed in the newly plastic area. The plastic deformation then extends from the ends of the cracks which increase until becoming visible with the naked eye, and lead to failure of the part. Fatigue damage is a cumulative phenomenon.

If the stress–strain cycle is plotted, the hysteresis loop obtained is an open curve whose form evolves depending on the number of applied cycles [FEO 69]. Each cycle of stress produces certain damage and the succession of the cycles results in a cumulative effect.

The damage is accompanied by modifications of the mechanical properties and, in particular, of a reduction of the static ultimate tensile strength R_m and of the fatigue limit strength.

This is generally local to the place of a geometrical discontinuity or a metallurgical defect. The fatigue damage is also related to metallurgical and mechanical phenomena, with the appearance and growth of cracks depending on the microstructural evolution and mechanical parameters (possibly with the effects of the environment).

The damage can be characterized by:

- evolution of a crack and energy absorption of plastic deformation in the plastic zone which exists at the ends of the crack;
- loss of strength in static tension;
- reduction of the fatigue limit stress up to a critical value corresponding to the failure; and
- variation of the plastic deformation which increases with the number of cycles up to a critical value.

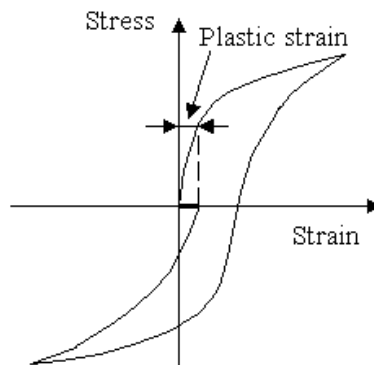


Figure 1.11. *Unclosed hysteresis loop*

We can suppose that fatigue is [COS 69]:

- the result of a dynamic variation of the conditions of load in a material;
- a statistical phenomenon;
- a cumulative phenomenon; and
- a function of material and of amplitude of the alternating stresses imposed on material.

There are several approaches to the problem of fatigue:

- establishing empirical relations taking experimental results into account;
- expressing in an equation the physical phenomena in the material, including microscopic cracks starting from intrusion defects and propagation of these microscopic cracks until macro-cracks and failure are obtained.

Cazaud *et al.* [CAZ 69] quote several theories concerning fatigue, the principal theories being:

- mechanical theories;
 - theory of the secondary effects (consideration of the homogeneity of the material, regularity of the distribution of the effort);
 - theory of hysteresis of pseudo-elastic deformations (discussion based on Hooke's law);
 - theory of molecular slip,
 - theory of work hardening,
 - theory of crack propagation, and
 - theory of internal damping;
 - physical theories, which consider the formation and propagation of the cracks using models of dislocation starting from extrusions and intrusions;
 - static theories, in which the stochastic character of the results is explained by the heterogeneity of materials, the distribution of the stress levels, cyclic character of loading, etc.;
 - theories of damage; and
 - low-cycle plastic fatigue, in the case of failures caused by approximately $N < 10^4$ cycles.

The estimate of the lifetime of a test bar is carried out from:

- a curve characteristic of the material (which gives the number of cycles to failure according to the amplitude of stress), in general sinusoidal with zero mean (S-N curve); and
- a law of accumulation of damages.

The various elaborated theories are distinguished by the selected analytical expression to represent the curve of damage and the by the manner of cumulating the damages.

To avoid failures of parts by fatigue dimensioned in statics and subjected to variable loads, we were initially tempted to adopt arbitrary *safety factors*. If badly selected, i.e. insufficient or too large, these could lead to excessive dimensions and masses.

An ideal design would require use of materials in the elastic range. Unfortunately, the plastic deformations always exist at points of strong stress

concentration. The nominal deformations and stresses are elastic and linearly related to the applied loads. This is not the case for stresses and local deformations which exist in metal at critical points, and which control resistance to fatigue of the whole structure.

It therefore proved necessary to carry out tests on test bars for better estimating of the resistance to fatigue under dynamic load, beginning with the simplest, i.e. the sinusoidal load. We will see in the following chapters how the effects of random vibrations most frequently met in practice can be evaluated.

1.4. Characterization of endurance of materials

1.4.1. *S-N curve*

The endurance of materials is studied in the laboratory by subjecting test bars cut in the material to be studied to stresses (or strains) of amplitude σ until rupture, generally sinusoidal with zero mean.

Following the work of Wöhler [WÖH 60], [WÖH 70] carried out on axes of trucks subjected to rotary bending stresses, we note that for each test bar, the number N of cycles to failure (*endurance of the part* or *fatigue life*) depends on σ . The curve obtained in plotting σ against N is termed the *S-N curve* (stress versus number of cycles) or *Wöhler's curve* or *endurance curve*. The endurance is therefore the ability of a machine part to resist fatigue.

Taking into account the huge variations of N with σ , it is usual to plot $\log N$ (decimal logarithm in general) on abscissae. Logarithmic scales on abscissae and on ordinates are also sometimes used.

This curve is generally composed of three zones [FAC 72], [RAB 80] (Figure 1.12):

– zone AB: corresponding to *low-cycle fatigue*, which corresponds to the largest stresses higher than the yield stress of material, where N varies from one-quarter of cycle with approximately 10^4 to 10^5 cycles (for mild steels). In this zone, we observe significant plastic deformation followed by failure of the test bar. The plastic deformation ε_p can be related here to the number of cycles to the failure by a simple relationship of the form:

$$N^k \varepsilon_p = C \quad [1.16]$$

where the exponent k is close to 0.5 for common metals (steels, light alloys) [COF 62].

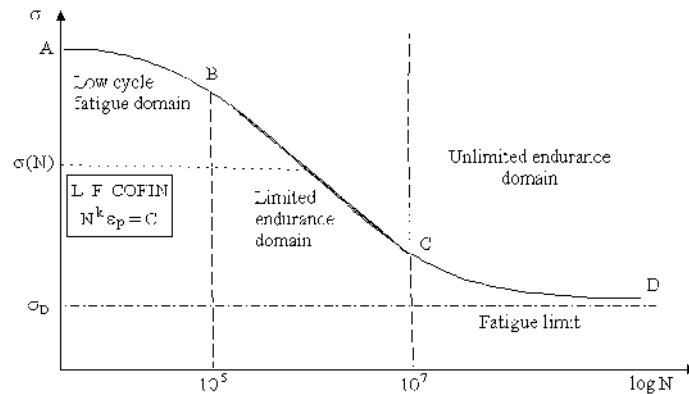


Figure 1.12. Main zones of the S-N curve

– zone BC: often approximates a straight line on log-linear scales (or sometimes on log-log scales), in which the fracture certainly appears under a stress lower than previously, without the appearance of measurable plastic deformation. There are many relationships proposed between σ and N to represent the phenomenon in this domain where N increases and when σ decreases. This zone, known as the *zone of limited endurance*, lies between approximately 10^4 cycles and 10^6 to 10^7 cycles.

– zone CD: where D is a point which, for ferrous metals, is *ad infinitum*. The S-N curve generally presents a significant variation of slope around 10^6 to 10^7 cycles, followed in a clear way to a greater or lesser extent, marked by a zone (CD) where the curve tends towards a limit parallel with the N axis. On this side of this limit, the value of σ is denoted σ_D ; there is never failure by fatigue whatever the number of cycles applied. σ_D is referred to as the *fatigue limit* and represents the stress with zero mean of greater amplitude for which we do not observe failure by fatigue after an infinite number of cycles. This stress limit does not exist or can be badly defined for certain materials [MEG 00], [NEL 78] (e.g. high-strength steels, non-ferrous metals).

For sufficiently resistant metals, where it is not possible to evaluate the number of cycles which the test bar would support without damage [CAZ 69] (too large a test duration) and to take account of the scatter of the results, the concept of conventional fatigue limit or endurance limit is introduced. It is about the greatest amplitude of stress σ for which 50% of failures after N cycles of stress is observed.

It is denoted $\sigma_m = 0$, $\sigma_D(N)$. N can vary between 10^6 and 10^8 cycles [BRA 80a, b]. For steels, $N = 10^7$ and $\sigma_D(10^7) \approx \sigma_D$. The notation σ_D is used in this case.

NOTE.–

Brittle materials do not have a well-defined fatigue limit [BRA 81], [FID 75].

For extra-hardened tempered steels (certainly titanium, copper or aluminum alloys), or when there is corrosion, this limit remains theoretical and without interest since the fatigue life is never infinite.

When the mean stress σ_m is different from zero, it is important to associate σ_m with the amplitude of the alternating stress. The fatigue limit can be written σ_a or σ_{aD} in this case.

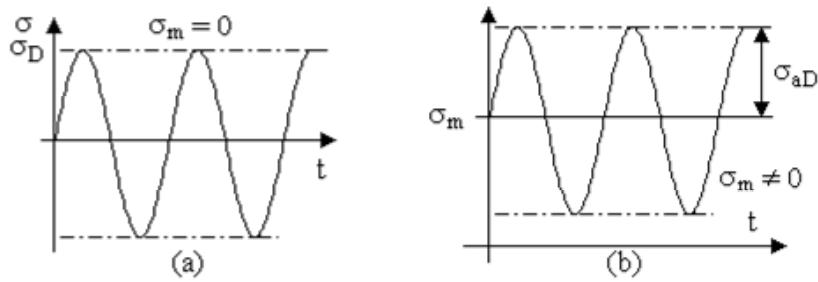


Figure 1.13. Sinusoidal stress with (a) zero and (b) non-zero mean

Definition

The *endurance ratio* is the ratio of the fatigue limit σ_D (normally at 10^7 cycles) to the ultimate tensile strength R_m of material:

$$R = \frac{\sigma_D(N)}{R_m} \quad [1.17]$$

NOTE.–

The S-N curve is sometimes plotted on reduced scales on axes (σ/R_m , N), in order to be able to proceed more easily to comparisons between different materials.

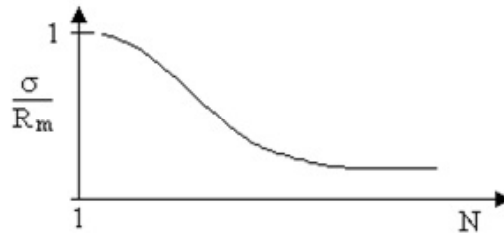


Figure 1.14. *S-N curve on reduced axes*

1.4.2. Influence of the average stress on the S-N curve

According to the value of the stress ratio R , the S-N curve has a different slope and intercept (Figure 1.15).

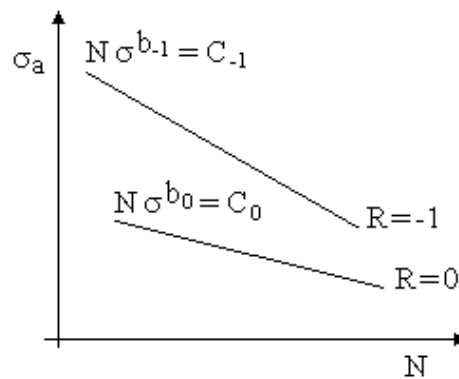


Figure 1.15. *Influence of the stress ratio*

K. Gołoś and S. Esthewi [GOL 97] define an “influence coefficient” aimed to take into account the influence of the average stress. This coefficient $\Psi(N)$ is function of the number of cycles to fracture N . It is written

$$\Psi(N) = \eta N^\lambda \quad [1.18]$$

where η and λ are experimental parameters determined during tests carried out with $R = 0$ and $R = -1$.

$\Psi(N)$ is determined from the slope of the curves in the Haigh diagram (Figure 1.16) [PAW 00].

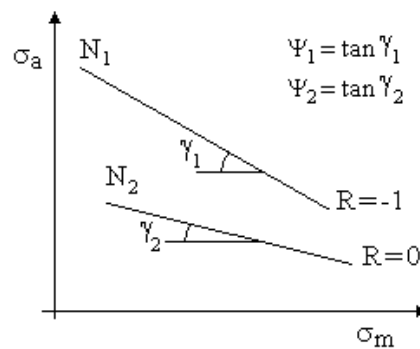


Figure 1.16. Haigh diagram – calculation of the influence coefficient

1.4.3. Statistical aspect

The S-N curve of a material is plotted by successively subjecting ten (or more) test bars to sinusoidal stresses of various amplitudes. The results show that there is considerable scatter in the results, in particular for the long fatigue lives. For a given stress level, the relationship between the maximum and the minimal value of the number of cycles to failure can exceed 10 [ROO 69], [NEL 78].

The dispersion of the results is related on the heterogeneity of materials, the surface defects, the machining tolerances and, in particular, to metallurgical factors. Among these factors, inclusions are most important. Scatter is in fact due to the action of fatigue in a metal, which is generally strongly localized. Contrary to the case of static loads, only a small volume of material is concerned. The rate of fatigue depends on the size, orientation and chemical composition of some material grains which are located in a critical zone [BRA 80b], [LEV 55], [WIR 76].

In practice, it is therefore not realistic to characterize the resistance to fatigue of a material by a S-N curve plotted from only one fatigue test at each stress level. It is more correct to describe this behavior by a curve in a statistical manner, the

abscissae providing the endurance N_p for a survival of p percent of the test bars [BAS 75], [COS 69].

The median endurance curve (or *equiprobability curve*) denoted N_{50} (i.e. survival of 50% of the test bars), or sometimes the median curves with ± 1 to 3 standard deviations or other isoprobability curves, are generally given [ING 27].

Without other indication, the S-N curve is the median curve.

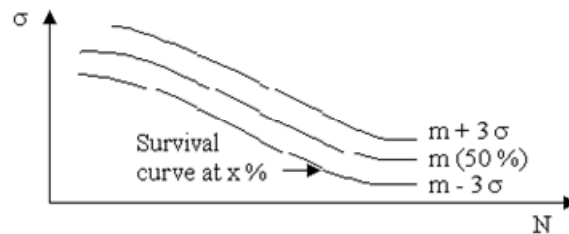


Figure 1.17. *Isoprobability S-N curves*

NOTE.— *The scatter of fatigue life of non-ferrous metals (aluminum, copper, etc.) is less than that of steels, probably because these metals have fewer inclusions and inhomogenities.*

1.4.4. *Distribution laws of endurance*

For high stress levels, endurance N follows a log-normal law [DOL 59], [IMP 65]. In other words, in scales where the abscissa carry $\log N$, the distribution of $\log N$ follows, in this stress domain, a roughly normal law (nearer to the normal law when σ is higher) with a scatter which decreases when σ increases. M. Matolcsy [MAT 69] considers that the standard deviation s can be related to the fatigue life at 50% by an expression of the form

$$s(N) = A N_{50}^{\beta} \quad [1.19]$$

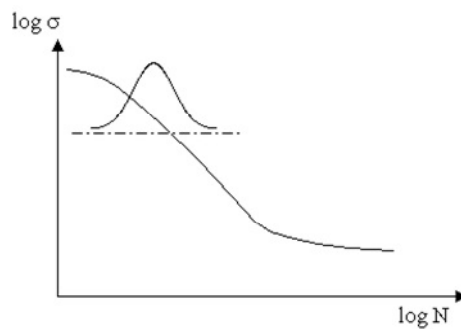
where A and β are constant functions of material.

Example 1.1.

	β
Aluminum alloys	1.125
Steels	1.114–1.155
Copper wires	1.160
Rubber	1.125

Table 1.2. *Examples of values of the exponent β*

G.M. Sinclair and T.J. Dolan [SIN 53] observed that the statistical law describing the fatigue evolution is roughly log-normal and that the standard deviation of the variable ($\log N$) varies with the amplitude of the applied stress according to an exponential law.

**Figure 1.18.** *Log-normal distribution of the fatigue life*

In the endurance zone, close to σ_D , F. Bastenaire [BAS 75] showed that the inverse $1/N$ of endurance follows a modified normal law (with truncated tail).

Other statistical models were proposed e.g. following [YAO 72], [YAO 74]:

- the normal law [AST 63];
- extreme value distribution;
- Weibull's law [FRE 53]; and
- the gamma law [EUG 65].

From a compilation of various experimental results, P.H. Wirshing [WIR 81] checked that, for welded tubular parts, the log-normal law is that which adapts best. It is this law which is most often used [WIR 81]. It has the following advantages:

- well-defined statistical properties;
- easy to use; and
- adapts to large variations in coefficient.

Tables 1.3 and 1.4 give values of the variation coefficient of the number of cycles to failure for some materials noted in the literature [LAL 87].

Value 0.2 of the standard deviation (on log N) is often used for the calculation of the fatigue lives (for notched or other parts) [FOR 61], [LIG 80], [LUN 64], [MEH 53].

Authors	Materials	Conditions	V_N (%)
Whittaker and Besuner [WHIT 69]	Steels $R_m \leq 1650$ MPa (240 ksi)		36
	Steels $R_m > 1650$ MPa (240 ksi)		48
	Aluminum alloy		27
	Alloy titanium		36
			(Log-normal)
Endo and Morrow [END 67] [WIR 82]	Steel 4340	Low-cycle fatigue ($N < 10^3$)	14.7
	7075-T6		17.6
	2024-T4		19.7
	Titanium 811		65.8
Swanson [SWA 68]	Steel SAE 1006	Fatigue under narrow band random noise	25.1
	Maraging steel 200 grade		38.6
	Maraging steel Nickel 18%		69.0
Gurney [GUR 68]	Welded structures	Mean	52

Table 1.3. Examples of values of the variation coefficient of the number of cycles to failure

1.4.5. Distribution laws of fatigue strength

Another way of resolving the problem consists of studying *the fatigue strength* of the material [SCH 74], i.e. the stress which the material can resist during N cycles. This strength also has a statistical character; strength to p percent of survival and a median strength are also defined here.

The *response curve* represents the probability of failure during a test with duration limited to N cycles, depending on the stress σ [CAZ 69], [ING 27].

The experiment shows that the fatigue strength follows a roughly normal law whatever the value of N and is fairly independent of N [BAR 77]. This constancy is masked on the S-N diagrams by the choice of the log-linear or log-log scales, scatter appearing to increase with N. Some values of the variation coefficient of this law for various materials, extracted from the literature, can be found in [LAL 87].

Authors	Materials	Conditions	V_N (%)
Blake and Baird [BLA 69]	Aerospace components	Random loads	3 to 30
Epreman and Mehl [EPR 52]	Steels Log-normal law	s_{\log}/m_{\log}	2.04 to 8.81 Log-normal law
Ang and Munse [Ang 75]	Welding		52
Whittaker [WHIT 72]	Steel UTS \leq 1650 MPa		36
	Steel UTS $>$ 1650 MPa		48
	Aluminum alloys		22
	Titanium alloys		36
Wirsching [WIR 83b]	Welding (tubes)		70 to 150

Wirsching and Wu [WIR 83c]	RQC - 100 Q	Plastic strain	15 to 30
		Elastic strain	55
	Waspaloy B	Plastic strain	42
	Super alloys Containing Nickel	Elastic strain	55
Wirsching [WIR 83a]	V_N , often about 30% to 40%, can reach 75% and even exceed 100%. Low-cycle fatigue field: 20% to 40% for the majority of metal alloys. For N large, V_N can exceed 100%.		
Yokobori [YOK 65]	Steel	Rotational bending or traction compression	28 to 130
Dolan and Brown [DOL 52]	Aluminum alloy 7075.T6	Rotational bending	44 to 80
Sinclair and Dolan [SIN 53]	Aluminum alloy 75.S-T	Rotational bending	10 to 100
Levy [LEV 55]	Mild steel	Rotational bending	43 to 75
Konishi and Shinozuka [KON 56]	Notched plates - Steel SS41	Alternate traction	18 to 43
Matolsy [MAT 69]	Synthesis of various test results		20 to 90
Tanaka and Akita [TAN 72]	Silver/nickel wires	Alternating bending	16 to 21

Table 1.4. Examples of values of the variation coefficient of the number of cycles to failure

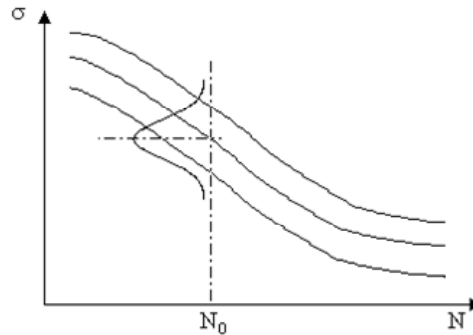


Figure 1.19. Gaussian distribution of fatigue strength

Authors	Materials	Parameter	V_N (%)
Ligeron [LIG 80]	Steels Various alloys	Fatigue limit stress	4.4 to 9.4
Yokobori [YOK 65]	Mild steel	Fatigue limit stress	2.5 to 11.3
Mehle [MEH 53]	Steel SAE 4340		20 to 95
Epreman [WIR 83a]	Large variety of metallic materials	Endurance stress (failure for given N)	5 to 15

Table 1.5. Examples of values of the variation coefficient of the endurance strength for a given N

For all the metals, J.E. Shigley [SHI 72] proposes a variation coefficient σ_D (ratio of the standard deviation to the mean) equal to 0.08 [LIG 80], a value which can be reduced to 0.06 for steels [RAN 49].

1.4.6. Relation between fatigue limit and static properties of materials

Some authors tried to establish empirical formulae relating the fatigue limit σ_D and its standard deviation to the mechanical characteristics of the material (Poisson coefficient, Young's modulus, etc.). For example, the relations listed in Table 1.6 were proposed for steels [CAZ 69], [LIE 80].

After completing a large number of fatigue tests (rotational bending, on test bars without notches). A. Brand and R. Sutterlin [BRA 80a] noted that the best correlation between σ_D and a mechanical strength parameter is that obtained with the ultimate strength R_m (tension):

$$\sigma_{D50\%} = R_m \left(0.57 - 1.2 \cdot 10^{-4} R_m \right) \text{ for } 800 \leq R_m \leq 1300 \text{ N/mm}^2$$

$$\sigma_D = R_m \left(0.56 - 1.4 \cdot 10^{-4} R_m \right) \text{ for } R_m < 800 \text{ N/mm}^2 \text{ or } R_m > 1300 \text{ N/mm}^2$$

All these relations only correctly represent the results of the experiments which made it possible to establish them, and therefore are not general. A. Brand and R. Sutterlin [BRA 80a] tried, however, to determine a more general relation, independent of the size of the test bars and stress, of the form:

$$\sigma_{DM} = a \log \chi + b$$

where a and b are related to R_m . σ_{DM} is the real fatigue limit related to the nominal fatigue limit σ_{Dnom} by

$$\sigma_{DM} = K_t \sigma_{Dnom}$$

where K_t = stress concentration factor. χ is the stress gradient, defined as the value of the slope of the tangent of the stress field at the notch root divided by the maximum value of the stress at the same point, i.e.

$$\chi = \lim_{x \rightarrow 0} \frac{1}{\sigma} \frac{d\sigma}{dx}$$

The variation coefficient is defined:

$$v = \frac{s_{\sigma_D}}{\bar{\sigma}_D} = 6 \%$$

where v is independent of R_m . A. Brand and R. Sutterlin [BRA 80a] recommend a value of 10%.

Houdremont and Mailander	$\sigma_D = 0.25 (R_e + R_m) + 5$	R_e = yield stress R_m = ultimate stress
Lequis, Buchholtz and Schultz	$\sigma_D = 0.175 (R_e + R_m - A\% + 100)$	$A\%$ = lengthening, in percent.
Fry, Kessner and Öttel	$\sigma_D = \alpha R_m + \beta R_e$	α proportional to R_m and β inversely proportional
Heywood	$\sigma_D = \frac{R_m}{2}$ $\sigma_D = 150 + 0.43 R_e$	
Brand	$\sigma_D = 0.32 R_m + 121$	
Lieurade and Buthod [LIE 82]	$\sigma_D = 0.37 R_m + 77$ $\sigma_D = 0.38 R_m + 16$ $\sigma_D = 0.41 R_m + 2 A$ $\sigma_D = 0.39 R_m + S$	(to 15% near) S = striction, expressed in %
Jüger	$\sigma_D = 0.2 (R_e + R_m + S)$	
Rogers	$\sigma_D = 0.4 R_e + 0.25 R_m$	
Mailander	$\sigma_D = (0.49 \pm 20\%) R_m$ $\sigma_D = (0.65 \pm 30\%) R_e$	
Stribeck	$\sigma_D = (0.285 \pm 20\%) (R_e + R_m)$	
In all the above relations, σ_D , R_m and R_e are expressed in N / mm^2 .		
Feodossiev [FEO 69]	Steel, bending: $\sigma_D \approx 0.4$ to $0.5 R_m$ Very resistant steels: $\sigma_D \approx 4000 + \frac{1}{6} R_m$ (in kg / cm^2) Non-ferrous metals: $\sigma_D \approx 0.25$ to $0.5 R_m$	

Table 1.6. Examples of relations between the fatigue limit and the static properties of materials

1.4.7. Analytical representations of S-N curve

Various expressions have been proposed to describe the S-N curve representative of the fatigue strength of a material, often in the limited endurance domain (the definition of this curve has evolved over the years from a deterministic curve to a curve of statistical character).

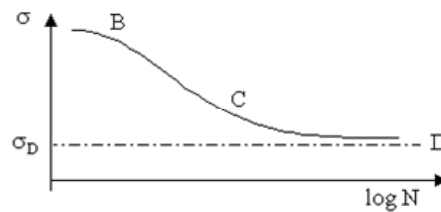


Figure 1.20. Representation of the S-N curve in semi-logarithmic scales

The S-N curve is generally plotted in semi-logarithmic scales of $\log N$ and σ , in which it presents a roughly linear part (around an inflection point), a curve characteristic of the material (BC) and an asymptote to the straight line $\sigma = \sigma_D$.

Among the many more or less complicated representations (none of which are really general), the following relations can be found [BAS 75], [DEN 71], [LIE 80].

1.4.7.1. Wöhler relation

$$\sigma = \alpha - \beta \log N \quad [1.20]$$

This relation does not describe the totality of the curve since σ does not tend towards a limit σ_D when $N \rightarrow \infty$ [HAI 78]. It represents only the part BC. It can also be written in the form [WÖH 70]:

$$N e^{a\sigma} = b \quad [1.21]$$

1.4.7.2. Basquin relation

The relation suggested by Basquin in 1910 [BAS 10] is of the form

$$\ln \sigma = \alpha - \beta \ln N \quad [1.22]$$

i.e.

$$N \sigma^b = C \quad [1.23]$$

where

$$\beta = \frac{1}{b} \text{ and } \ln C = \frac{\alpha}{\beta}$$

The parameter b is sometimes referred to as the *index of the fatigue curve* [BOL 84].

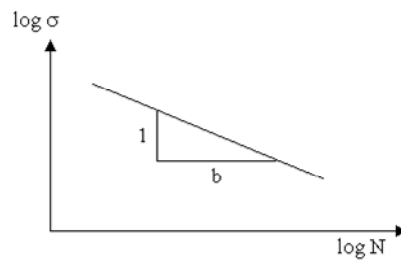


Figure 1.21. Significance of the parameter b of Basquin's relation

In these scales, the curve can be entirely linearized (upwards) by considering the amplitudes of the true stresses (and neither nominal). Expression [1.23] can also be written:

$$\sigma = \sigma_{RF} N^\beta \quad [1.24]$$

or

$$N \sigma^b = \sigma_{RF}^b \quad [1.25]$$

where σ_{RF} is the fatigue strength coefficient. This expression is generally valid for high values of N ($> 10^4$). If there is a non-zero σ_0 mean stress, constant C must be replaced by:

$$C \left(1 - \frac{\sigma_0}{R_m} \right)^m$$

where C is the constant used when $\sigma_0 = 0$ and R_m is the ultimate strength of the material [WIR 83a].

In the expression $N \sigma^b = C$, the stress tends towards zero when N tends towards the infinite. This relation is therefore representative of the S-N curve only for part BC. In addition, it represents a straight line in logarithmic scales and not in semi-logarithmic scales (log-linear). A certain number of authors presented the results of the fatigue tests in these scales (log-log) and showed that part BC is close to a straight line [MUR 52]. F.R. Shanley [SHA 52] considers in particular that it is preferable to choose these scales. H.P. Lieurade [LIE 80] notes that the representation of Basquin is less appropriate than that of the relation of Wöhler in the intermediate zone, and that the Basquin method is not better around the fatigue limit. It is very much used, however.

To take account of the stochastic nature of this curve, P.H. Wirsching [WIR 79] proposed treating constant C like a log-normal random variable of mean \bar{C} and standard deviation σ_C and provides the following values, in the domain of the great numbers of cycles:

- median: $1.55 \cdot 10^{12}$ (ksi)⁽¹⁾,
- variation coefficient: 1.36

(statistical study of S-N curves relating to connections between tubes).

Some numerical values of the parameter b in Basquin's relationship

Metals. The range of variation of b is 3–25. The most common values are between 3 and 10 [LEN 68]. M. Gertel [GER 61], [GER 62] and C.E. Crede and E.J. Lunney [CRE 56b] consider a value of 9 to be representative of most materials. It is probably a consideration of this order that led to the choice of 9 by standards such as MIL-STD-810, AIR, etc. This choice is satisfactory for most light alloys and copper but may be unsuitable for other materials. For instance, for steel, the value of b varies between 10 and 14 depending on the alloy. D.S. Steinberg [STE 73] mentions the case of 6144-T4 aluminum alloy for which $b = 14$ ($N \sigma^{14} = 2.26 \cdot 10^{78}$).

b is approximately 9 for ductile materials and approximately 20 for brittle materials, whatever the ultimate strength of the material [LAM 80].

¹ 1 ksi = 6.8947 MPa

Material	Type of fatigue test	$\frac{\sigma_{\min}}{\sigma_{\max}}$	b
2024-T3 aluminum	Axial load	-1	5.6
2024-T4 aluminum	Rotating beam	-1	6.4
7075-T6 aluminum	Axial loading	-1	5.5
6061-T6 aluminum	Rotating beam	-1	7.0
ZK-60 magnesium			4.8
BK31XA-T6 magnesium	Axial load	0.25	8.5
	Rotating beam	-1	5.8
QE 22-T6 magnesium	Wöhler	-1	3.1
4130 steel			
Standardized	Axial load	-1	4.5
Hardened	Axial load	-1	4.1
6Al-4V Ti	Axial load	-1	4.9
Beryllium			
Hot pressed	Axial load	0	10.8
Block		0.2	8.7
		-1	12.6
Cross Rol Sheat	Axial load	0.2	9.4
Invar	Axial load		4.6
Anneal copper			11.2
1S1 fiberglass			6.7

Table 1.7. Examples of values of the parameter b [DEI 72]

The lowest values indicate that the fatigue strength drops faster when the number of cycles is increased, which is generally the case for the most severe geometric shapes. The lower the stress concentration, the higher the value of parameter b. Table 1.7 gives the value of b for a few materials according to the type of load applied: tension-compression, torsion, etc. and the value of the mean stress, i.e. the ratio $\sigma_{\min}/\sigma_{\max}$.

A few other values are given by R.G. Lambert [LAM 80] with no indication of the test conditions.

Material	b
Copper wire	9.28
Aluminum alloy 6061-T6	8.92
7075-T6	9.65
Soft solder (63-37 Tin - Lead)	9.85
Steel 4340 (BHN 243)	10.5
Steel 4340 (BHN 350)	13.2
Nickel IN-718	16.67
AZ31B Magnesium alloy	22.4

Table 1.8. Examples of values of the parameter *b* [LAM 80]

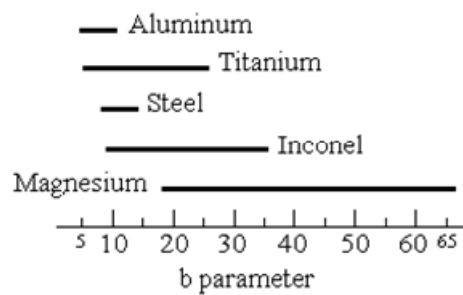


Figure 1.22. Examples of values of the parameter *b* [CAR 74]

It should be noted that the *b* parameter of an assembly can differ appreciably from that of the material of which it is composed. The *b* parameter defined in experiments for a steel ball bearing is, for example, close to 4. That of steel or aluminum welded parts has a *b* value between 3 and 6 [BSI 80], [EUR 93], [HAA 98], [LAS 05], [MAN 04], [SHE 05], [TVE 03].

It is therefore necessary to be very cautious when choosing the value of this parameter, especially when reducing the test times for constant fatigue damage testing.

Case of electronic components

The failures observed in electronic components follow the conventional fatigue failure model [HAS 64]. The equations established for structures are therefore applicable [BLA 78]. During initial tests on components such as capacitors, vacuum tubes, resistors, etc. and on equipment, it was observed that the failures (lead breakage) generally occurred near the frame resonance frequencies, generally below 500 Hz [JAC 56]. The analysis of tests conducted on components by D.L. Wrisley and W.S. Knowles [WRI] tends to confirm the existence of a fatigue limit.

Electronic components could be expected *a priori* to be characterized by a parameter b of around 8 or 9 for fatigue strength, at least in the case of discrete components with copper or light alloy leads. That is the value chosen by some authors [CZE 78].

Few pieces of data have been published on the fatigue strength of electronic components. C.A. Golueke [GOL 58] provides S-N curves plotted from the results of fatigue testing conducted at resonance on resistors, for setups such that the resonance frequency is between 120 Hz and 690 Hz. Its results show that the S-N curves obtained for each resonance are roughly parallel. On $\log N - \log \ddot{x}$ scales (acceleration), parameter b is very close to 2. Components with the highest resonance frequency have the longest life expectancy, which demonstrates the interest of decreasing the component lead length to a minimum.

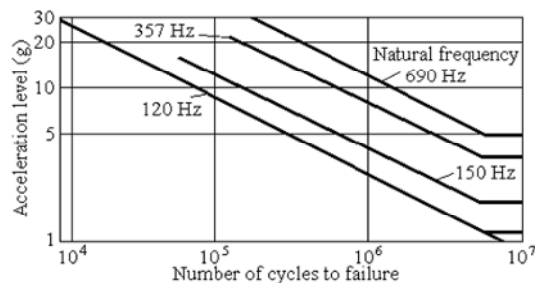


Figure 1.23. Examples of S-N curves of electronic components [GOL 58]

This work also reports that the most fragile parts regarding fatigue strength are the soldered joints and interconnections followed by capacitors, vacuum tubes, relays to a much lesser extent, transformers and switches.

M. Gertel [GER 61], [GER 62] writes the Basquin relation $N \sigma^b = C$ in the form

$$N \frac{\sigma^b}{\sigma_D^b} = \frac{C}{\sigma_D^b} = C_1 \quad [1.26]$$

where σ_D is the fatigue limit. If the excitation is sinusoidal [GER 61] and if the structure, comparable to a one-degree-of-freedom system, is subjected to tension-compression, the movement of mass m is such that

$$m \ddot{y} = \sigma S \quad [1.27]$$

where σ is stress in the part with cross-section S . If the structure is excited at resonance, we have:

$$\ddot{y} = Q \ddot{x} \quad [1.28]$$

and

$$\ddot{x} = \frac{\sigma S}{m Q} \quad [1.29]$$

Knowing that the specific damping energy D is related to the stress by

$$D = J \sigma^n \begin{cases} n = 2.4 & \text{if } \sigma \leq 0.8 R_e \\ n = 8 & \text{if } \sigma > 0.8 R_e \end{cases} \quad [1.30]$$

and that the Q factor can be considered as the product:

$$Q = K_m K_v \quad [1.31]$$

where

$$K_m = \frac{\pi \sigma^2}{E D}$$

is the dimensionless factor of the material, E is Young's modulus, and where K_v is the dimensionless volumetric stress factor, we obtain

$$\ddot{x} = \frac{S \sigma}{m K_v K_m} = \frac{S \sigma}{m K_v} \frac{E D}{\pi \sigma^2}$$

$$\ddot{x} = \frac{S E}{m K_v \pi} J \sigma^n$$

$$\ddot{x} = \frac{S E J}{m K_v \pi} \sigma^{n-1} \quad [1.32]$$

If

$$\ddot{x}_e = \frac{S E J}{m K_v \pi} R_e^{n-1}$$

$$\frac{\ddot{x}}{\ddot{x}_e} = \left(\frac{\sigma}{R_e} \right)^{n-1}$$

and

$$N \frac{\sigma^b}{R_e^b} = C_1,$$

we obtain

$$N \left(\frac{\ddot{x}}{\ddot{x}_e} \right)^{\frac{b}{n-1}} = C_1, \quad [1.33]$$

yielding the value of the parameter b of resistors in N - σ axes (instead of N , \ddot{x}):

$$b = 2(n-1) \quad [1.34]$$

which, for $n = 2.4$, is equal to $2 \times 1.4 = 2.8$. These low values of b are confirmed by other authors [CRE 56b], [CRE 57], [LUN 58]. Some relate to different

component technologies [DEW 86], [PER 08]. Among the published values are, for instance:

Resistors: b = 2.4 to 5.8 Vacuum tubes: b = 0.6	C.E. Crede [GER 61], [GER 62]
Capacitors: b = 3.6 (leads) Vacuum tubes: b = 2.83 to 2.13	E.J. Lunney and C.E. Crede [CRE 56b]
Circuit boards - Electric fault, then failure: b = 3 to 6	J. De Winne [DEW 86]
Electronic equipment (assumes copper wire) b=2.4 Complex electrical and electronic equipment items b =4.0	W. O. Hughes and M. E. McNelis [HUG 04]
Weldings b = 5.7	H.S. Gopalakrishna and J. Metcalf [GOP 89]
Electrical contact failures b = 4	D.S. Steinberg [STE 00]

Table 1.9. Some values of b parameter

1.4.7.3. *Some other laws*

Other laws include that of C.E. Stromeyer [STR 14]:

$$\log(\sigma - \sigma_D) = \alpha - \beta \log N \quad [1.35]$$

40 Fatigue Damage

or

$$\sigma = \sigma_D + \left(\frac{C}{N} \right)^{1/b} \quad [1.36]$$

or

$$(\sigma - \sigma_D)^b N = C \quad [1.37]$$

Here, σ tends towards σ_D when N tends towards infinity.

A. Palmgren [PAL 24] stated that

$$\sigma = \sigma_D + \left(\frac{C}{N + A} \right)^{1/b} \quad [1.38]$$

or

$$(\sigma - \sigma_D)^b (N + A) = C \quad [1.39]$$

a relation which is better adjusted using experimental curves than Stromeayer's relation.

According to W. Weibull [WEI 49],

$$\frac{\sigma - \sigma_D}{R_m - \sigma_D} = \left(\frac{C}{N + A} \right)^{1/b} \quad [1.40]$$

where R_m is the ultimate strength of studied material. This relation does not improve the preceding relation. It can be also written:

$$\sigma = \sigma_D + \frac{F}{(N + A)^{1/b}} \quad [1.41]$$

where F is a constant and A is the number of cycles (different from 1/4) corresponding to the ultimate stress [WEI 52]. It was used in other forms, such as:

$$\sigma - \sigma_D = \left(\frac{C}{N} \right)^{1/n} \quad [1.42]$$

with $n = 1$ [PRO 48], $n = 2$ [FER 55] and

$$\frac{\sigma - \sigma_D}{R_m - \sigma} = b N^{-a} \quad [1.43]$$

where a and b are constants [FUL 63].

According to Corson [MIL 82],

$$(\sigma - \sigma_D) A^{\sigma - \sigma_D} = \frac{C}{N} \quad [1.44]$$

Bastenaire [BAS 75] stated that:

$$(N + B) (\sigma - \sigma_D) e^{A(\sigma - \sigma_D)} = C \quad [1.45]$$

1.5. Factors of influence

1.5.1. General

A great number of parameters affect fatigue strength and hence the S-N curve. The fatigue limit of a test bar can therefore be expressed in the form [SHI 72]:

$$\sigma_D = K_{sc} K_s K_\theta K_f K_r K_v \sigma'_D \quad [1.46]$$

where σ'_D is the fatigue limit of a smooth test bar and where the other factors make it possible to take into account the following effects:

- K_{sc} scale effect
- K_s surface effect
- K_θ temperature effect
- K_f form effect (notches, holes, etc.)
- K_r reliability effect

K_v various effects (loading rate, type of load, corrosion, residual stresses, stress frequency, etc.)

These factors can be classified as follows [MIL 82]:

- factors depending on the conditions of load (type of loads: tension/compression, alternating bending, rotational bending, alternating torsion, etc.);
- geometrical factors (scale effect, shape, etc.);
- factors depending on the conditions of surface;
- factors of a metallurgical nature; and
- factors of environment (temperature, corrosion etc).

We examine some of these parameters in the following sections.

1.5.2. *Scale*

For the sake of simplicity and minimizing cost, the tests of characterization of strength to fatigue are carried out on small test bars. The tacit and fundamental assumption is that the damage processes apply both to the test bars and the complete structure. The use of the constants determined with test bars for the calculation of larger parts assumes that the scale factor has little influence.

A scale effect can appear when the diameter of the test bar is increased, involving an increase in the concerned volume of metal and in the surface of the part, and thus an increase in the probability of cracking. This scale effect has as its origins:

- mechanics: existence of a stress gradient in the surface layers of the part, variable according to dimensions, weaker for the large parts (case of the non-uniform loads, such as torsion or alternating bending);
- statistics: larger probability of existence of defects being able to start microscopic cracks in the large parts; and
- technological: surface quality and material heterogeneity.

It is noted in practice that the fatigue limit is smaller when the test bar is larger. With equal nominal stress, the greater the dimensions of a part, the greater its fatigue strength decreases [BRA 80b], [BRA 81], [EPR 52].

B.N. Leis [LEI 78] and B.N. Leis and D. Broek [LEI 81] demonstrated that, under conditions to ensure that similarity is respected strictly at the critical points (notch root, crack edges, etc.), precise structure fatigue life predictions can be made from laboratory test results. Satisfying conditions of similarity is sometimes difficult to achieve, however, since there is a lack of understanding of the factors controlling the process of damage rate.

1.5.3. Overloads

We will see that the order of application of loads of various amplitudes is an important parameter. It is observed in practice that:

1. For a smooth test bar, the effect of an overload leads to a reduction in the fatigue life. J. Kommers [KOM 45] showed that a material which was submitted to significant over-stress, then to under-stress, can break even if the final stress is lower than the initial fatigue limit. This is because the over-stress produces a reduction in the initial fatigue limit. By contrast, an initial under-stress increases the fatigue limit [GOU 24].

J.R. Fuller [FUL 63] noted that the S-N curve of a material which has undergone an overload turns in the clockwise direction with respect to the initial S-N curve, around a point located on the curve with ordinate of amplitude σ_1 of the overload.

The fatigue limit is reduced. If n_2 cycles are carried out on the level σ_2 after n_1 cycles at level σ_1 , the new S-N curve takes the position 3 (Figure 1.24).

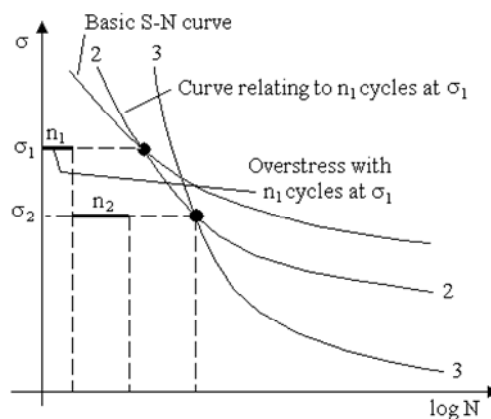


Figure 1.24. Rotation of the S-N curve of a material which has undergone an overload [FUL 63]

Rotation is quantitatively related to the value of the ratio n_1/N_1 on the over-stress level σ_1 . J.R. Fuller defines a *factor of distribution* which can be written for two load levels:

$$\beta = \frac{1}{q} \log_{10} \frac{10^q N_A}{N_A + N_a} = 1 + \frac{1}{q} \log_{10} \frac{N_A}{N_A + N_a} \quad [1.47]$$

where q is a constant generally equal to 3 (*notch sensitivity* of material to fatigue to the high loads), N_A is the number of cycles on the highest level σ_A and N_a is the number of cycles on the lower level σ_a .

If $\beta = 1$, all the stress cycles are carried out at the higher stress level ($N_a = 0$). This factor β enables the distribution of the peaks between the two limits σ_A and σ_a to be characterized and is used to correct the fatigue life of the test bars calculated under this type of load. It can be used for a narrowband random loading.

2. For a notched test bar, on which most of the fatigue life is devoted to the propagation of the cracks by fatigue, this same effect led to an increase in the fatigue life [MAT 71]. Conversely, an initial under-load accelerates cracking. This acceleration is all the more significant since the ensuing loads are larger. In the case of random vibrations, they are statistically not very frequent and of short duration so that the under-load effect can be neglected [WEI 78].

1.5.4. Frequency of stresses

The frequency, within reasonable limits of variation, is not important [DOL 57]. It is generally considered that this parameter has little influence as long as the heat created in the part can be dissipated and a heating does not occur which would affect the mechanical characteristics. (Stresses are considered here to be directly applied to the part with a given frequency. It is different when the stresses are due to the total response of a structure involving several modes [GRE 81]).

An assessment of the influence of the frequency shows [HON 83]:

- the results published are not always coherent, particularly because of corrosion effects;
- for certain materials, the frequency can be a significant factor when it varies greatly, acting differently depending on materials and load amplitude; and
- its effect is much more significant at high frequencies.

For the majority of steels and alloys, it is negligible for $f < 117$ Hz. In the low number of cycle fatigue domain, there is a linear relation between the fatigue life and the frequency on logarithmic scales [ECK 51]. Generally observed are:

- an increase in the fatigue limit when the frequency increases; and
- a maximum value of fatigue limit at a certain frequency.

For specific treatment of materials, unusual effects can be noted [BOO 70], [BRA 80b], [BRA 81], [ECK 51], [FOR 62], [FUL 63], [GUR 48], [HAR 61], [JEN 25], [KEN 82], [LOM 56], [MAS 66a], [MAT 69], [WAD 56], [WEB 66], [WHI 61]. I. Palfalvi [PAL 65] demonstrated theoretically the existence of a limiting frequency, beyond which the thermal release creates additional stresses and changes of state.

The effect of frequency seems more marked with the large numbers of cycles and decreases when the stress tends towards the fatigue limit [HAR 61]. It becomes paramount in the presence of a hostile environment (for example, corrosive medium, temperature) [LIE 91].

1.5.5. Types of stresses

The plots of the S-N curves are generally obtained by subjecting test bars to sinusoidal loads (tension and compression, torsion, etc.) with zero mean. It is also possible to plot these curves for random stress or even by applying repeated shocks.

1.5.6. Non-zero mean stress

Unless otherwise specified, it will be assumed in what follows that the S-N curve is defined by the median curve. The presence of a non-zero mean stress modifies the fatigue life of the test bar, in particular when this mean stress is relatively large compared to the alternating stress. A tensile mean stress decreases the fatigue life; a compressive stress increases it.

Since the amplitudes of the alternating stresses are relatively small in the fatigue tests with a great number of cycles, the effects of the mean stress are more important than in the tests with a low number of cycles [SHI 83].

If the stresses are large enough to produce significant repeated plastic strains, as in the case of fatigue with a small number of cycles, the mean strain is quickly released and its effect can be weak [TOP 69], [YAN 72].

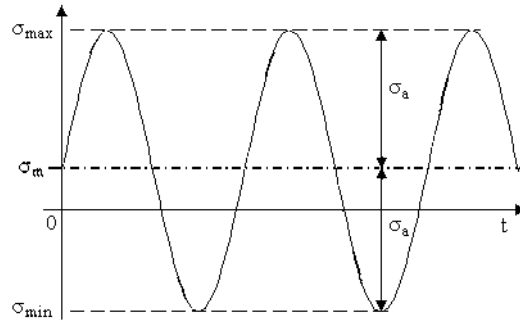


Figure 1.25. Sinusoidal stress with non-zero mean

When the mean stress σ_m is different from zero, the sinusoidal stress is generally characterized by two parameters from: σ_a , σ_{\max} , σ_{\min} and $R = \sigma_{\min}/\sigma_{\max}$.

Although this representation is seldom used, it is possible to use the traditional representation of the S-N curves with the logarithm of the number of cycles to failure on the abscissa axis and on the ordinate stress σ_{\max} , the curves being plotted for different values of σ_m or R [FID 75], [SCH 74].

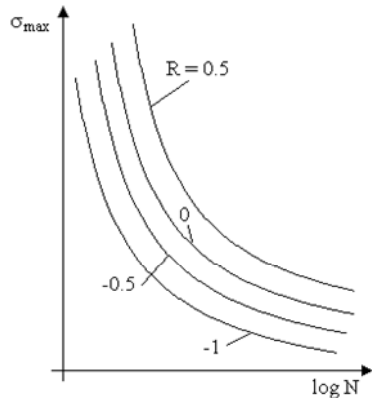


Figure 1.26. Representation of the S-N curves with non-zero mean versus R

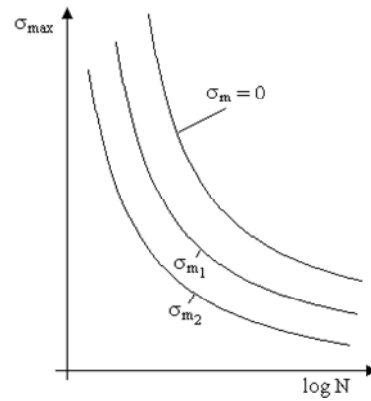


Figure 1.27. Representation of the S-N curves with non-zero mean versus the mean stress

Other authors plot S-N curves with σ_a versus N for various values of σ_m , and propose empirical relations between constants C and b of Basquin's relation ($N \sigma^b = C$) and σ_m [SEW 72]:

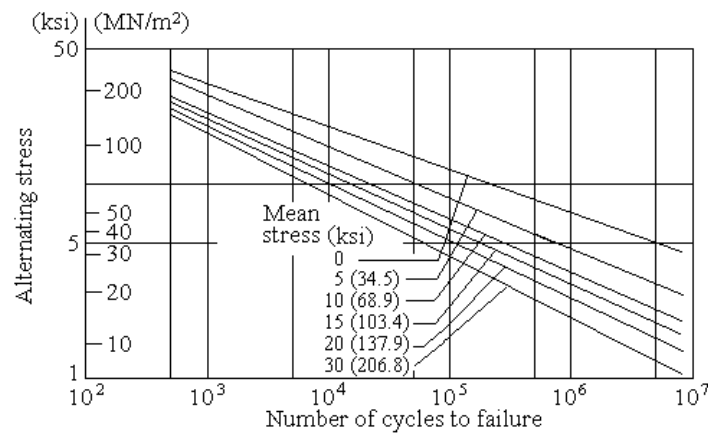


Figure 1.28. Example of S-N curves with non-zero mean

Example 1.2.

Aluminum alloy:

$$\log_{10} C = 9.45982 - 2.37677 \sigma_m + 1.18776 \sigma_m^2 - 0.25697 \sigma_m^3$$

$$b = 3.96687 - 0.213676 \sigma_m - 0.04786 \sigma_m^2 + 0.00657 \sigma_m^3$$

(σ_m in units of 10 ksi)⁽²⁾

It is generally agreed to use material below its yield stress ($\sigma_{\max} < R_e$) only, which limits the influence of σ_m on the lifespan. The application of static stress leads to a reduction in σ_a (for a material, a stress mode and a given fatigue life). It is therefore interesting to know how σ_a varies with σ_m . Several relations or diagrams were proposed to this end.

⁽²⁾ 1 ksi = 6.8947 MPa.

The locus of the fatigue limits observed during tests for various values of the couple (σ_m, σ_a) is an arc of curve crossing A and B. The domain delimited by arc AB and the two axes represents the couples (σ_m, σ_a) for which the fatigue life of the test bars is higher than the fatigue life corresponding to σ_D .

As long as $\sigma_{\max} (= \sigma_m + \sigma_a)$ remains lower than the yield stress R_e , the curve representing the variations of σ_a with σ_m is roughly a straight line. For $\sigma_{\max} \leq R_e$, we have, at the limit,

$$\sigma_{\max} = R_e = \sigma_m + \sigma_a$$

$$\sigma_a = R_e - \sigma_m.$$

This line crosses the axis $O\sigma_m$ at a point P on abscissa R_e and $O\sigma_a$ at a point Q on ordinate R_e . Let C be the point of $O\sigma_a$ having as ordinate $\sigma_{\max} (< R_e)$. The arc CB is the locus of the points (σ_m, σ_a) leading to the same fatigue life. This arc of curve crosses the straight line PQ at T. Only the arc (appreciably linear) crossing by T on the left of PQ is representative of the variations of σ_a varying with σ_m for $\sigma_{\max} \leq R_e$. On the right, the arc is no longer linear [SCH 74].

Curve AB has been represented by several analytical approximations, starting from the value of σ_D (for $\sigma_m = 0$), and from σ_a and σ_m , used to build this diagram *a priori* in an approximate way [BRA 80a], [GER 74], [GOO 30], [OSG 82], [SOD 30]:

– *Goodman line (1930)* modified by J. O. Smith [SMI 42] (1942):

$$\sigma_a = \sigma_D \left(1 - \frac{\sigma_m}{R_m} \right); \quad [1.48]$$

– *Söderberg line (1930)*:

$$\sigma_a = \sigma_D \left(1 - \frac{\sigma_m}{R_e} \right); \quad [1.49]$$

and

– Gerber parabola (1874):

$$\sigma_a = \sigma_D \left[1 - \left(\frac{\sigma_m}{R_m} \right)^2 \right] \quad [1.50]$$

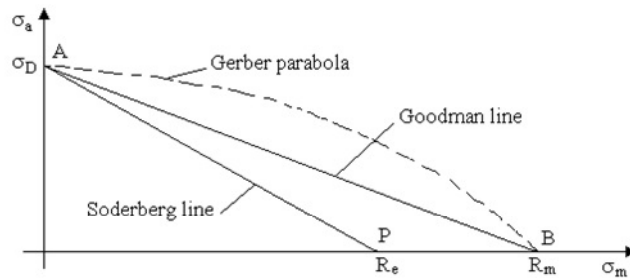


Figure 1.30. Haigh, Gerber, Goodman and Söderberg representations

The Haigh diagram is plotted for a given endurance N_0 , in general fixed at 10^7 cycles, but it can also be established for any number of cycles. In this case, curve CTB can similarly be represented depending on the case by:

Modified Goodman	Söderberg	Gerber
$\sigma_a = \sigma'_a \left(1 - \frac{\sigma_m}{R_m} \right) \quad [1.51]$	$\sigma_a = \sigma'_a \left(1 - \frac{\sigma_m}{R_e} \right) \quad [1.52]$	$\sigma_a = \sigma'_a \left[1 - \left(\frac{\sigma_m}{R_m} \right)^2 \right] \quad [1.53]$

These models make it possible to calculate the equivalent stress range $\Delta\sigma_{eq}$, taking into account the non-zero mean stress using the relation [SHI 83]:

$$\Delta\sigma_{eq} = \frac{1}{a} \Delta\sigma \quad [1.54]$$

where $\Delta\sigma$ is the total stress range, $a = 1 - \sigma_m/R_m$ (modified Goodman), σ_m is mean stress and R_m is ultimate tensile strength.

Relationships [1.51]–[1.53] can be written in the form

Modified Goodman	Söderberg	Gerber
$\frac{\sigma_a}{\sigma'_a} + \frac{\sigma_m}{R_m} = 1$ [1.55]	$\frac{\sigma_a}{\sigma'_a} + \frac{\sigma_m}{R_e} = 1$ [1.56]	$\frac{\sigma_a}{\sigma'_a} + \left(\frac{\sigma_m}{R_m}\right)^2 = 1$ [1.57]

The two most widely accepted methods are those of Goodman and Gerber. Experience has shown that test data tends to fall between the Goodman and Gerber curves. Goodman is often used due to mathematical simplicity and slightly conservative values.

Depending on materials, one of the representations is best suited. Nevertheless, the modified Goodman line is often considered too imprecise and leads to conservative results (it predicts lifetimes lower than real lifetimes) [HAU 69], [OSG 82], except close to the points $\sigma_m = 0$ and $R_m = 0$. It is good for brittle materials and conservative for ductile materials.

The Gerber representation was proposed to correct this conservatism; it adapts better to the experimental data for $\sigma_a > \sigma_m$. The case $\sigma_m \gg \sigma_a$ can correspond to plastic deformations. The model is worse for $\sigma_m < 0$ (compression). It is satisfactory for ductile materials.

The Söderberg model eliminates this latter problem, but it is more conservative than that of Goodman. It is used in applications where neither fatigue failure nor yielding should occur.

E.B. Haugen and J. A. Hritz [HAU 69] observe that:

- the modifications made by Langer (which exclude the area where the sum $\sigma_a + \sigma_m$ is higher than R_e) and by Sines are not significant;

- it is desirable to replace the static yield stress by the dynamic yield stress in this diagram; and

- the curves are not deterministic. It is preferable to use a Gerber parabola in statistical matter, of the form:

$$\frac{\sigma_a}{\bar{\sigma}_D} + \left(\frac{\sigma_m}{\bar{R}_m} \right)^2 = 1 \quad [1.58]$$

where $\bar{\sigma}_D$ and \bar{R}_m are mean values, like

$$\frac{\sigma_a}{\bar{\sigma}_D \pm 3 S_{\sigma_D}} + \left(\frac{\sigma_m}{\bar{R}_m \pm 3 S_{R_m}} \right)^2 = 1 \quad [1.59]$$

where S_{σ_D} and S_{R_m} are the standard deviations of σ_D and R_m , respectively [BAH 78].

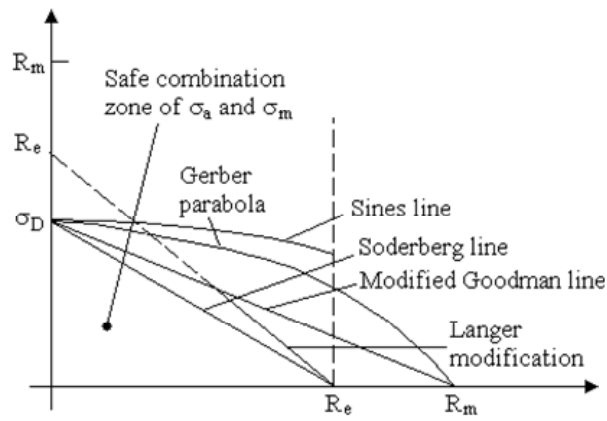


Figure 1.31. Haigh diagram. Langer and Sines modifications

NOTE.— The Haigh diagram can be built from the S-N curves plotted for several values of the mean stress σ_m (Figures 1.32 and 1.33)

A static test makes it possible to evaluate R_m . A test with zero mean stress yields σ'_a . For given N , the curves σ_{mi} have an ordinate equal to $\sigma_D(N)_i$.

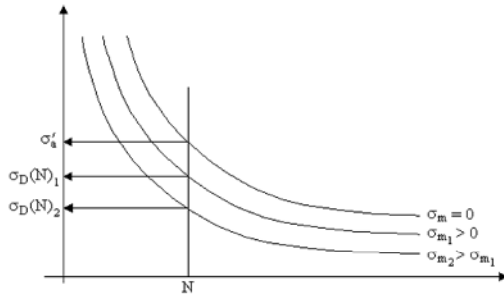


Figure 1.32. *S-N curves with non-zero mean stress, for construction of the Haigh diagram*

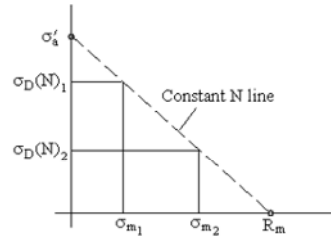


Figure 1.33. *Construction of the Haigh diagram*

Other relations

Von Settings-Hencky ellipse or Marin ellipse [MAR 56] is defined:

$$\left(\frac{\sigma_a}{\sigma'_a}\right)^2 + \left(\frac{\sigma_m}{R_m}\right)^2 = 1 \tag{1.60}$$

$$\frac{\sigma_a}{\sigma'_a} + \left(\frac{\sigma_m}{R_m}\right)^{ml} = 1 \tag{1.61}$$

where σ'_a is allowable stress when $\sigma_m = 0$, σ_a is allowable stress (for the same fatigue life N) for given $\sigma_m \neq 0$ and ml is a constant.

The case of $ml = 1$ (Goodman) is conservative. The experiment shows that $ml < 2$. A value of 1.5 is considered correct for the majority of steels [DES 75].

J. Bahuaud [MAR 56] states that:

$$\frac{\sigma_a}{\sigma_D} + \frac{1}{\rho} \left(\frac{\sigma_m}{R_t}\right)^2 + \left(1 - \frac{1}{\rho}\right) \frac{\sigma_m}{R_t} = 1 \tag{1.62}$$

where

$$\rho = \frac{R_{t \text{ compression}}}{R_{t \text{ tension}}}$$

and R_t is the true ultimate tensile and compressive strength.

If strength R_t is unknown, it can be approximated using

$$R_t = 0.92 R_m (1 + Z_u) \quad [1.63]$$

where Z_u is the striction coefficient and R_m is conventional ultimate strength.

According to Dietmann,

$$\left(\frac{\sigma_a}{\sigma_D} \right)^2 + \frac{\sigma_m}{R_m} = 1 \quad [1.64]$$

All these relations can be gathered in the more general form

$$\left(\frac{\sigma_a}{k_1 \sigma'_a} \right)^{r_1} + \left(\frac{\sigma_m}{k_2 R_m} \right)^{r_2} = 1 \quad [1.65]$$

where k_1 , k_2 , r_1 and r_2 are constant functions of the chosen law.

	r_1	r_2	k_1	k_2
Söderberg	1	1	1	R_e/R_m
Modified Goodman	1	1	1	1
Gerber	1	2	1	1
Von Mises-Hencky	2	2	1	1
Marin	1	ml	1	1

Table 1.10. Values of the constants of the general law (Haigh diagram)

NOTE.— In rotational bending, the following relation can be used in the absence of other data [BRA 80b]:

$$\sigma_{D \text{ rotative bending}} = \frac{\sigma_{D \text{ tension-compression}}}{0.9} \quad [1.66]$$

Morrow [MOR 68] proposes to amend Goodman's relationship for non-ferrous materials, using the true fracture strength σ_F (true fracture strength from a tension test) of the material instead of the ultimate strength R_m :

$$\frac{\sigma_a}{\sigma_a'} + \frac{\sigma_m}{\sigma_F} = 1 \quad [1.67]$$

Hence

$$\sigma_a = \sigma_a' \left(1 - \frac{\sigma_m}{\sigma_{fB}} \right) \quad [1.68]$$

As a second alternative, Morrow also proposed to change the true fracture strength with the strength to fracture coefficient σ_f' from the stress-life curve the stress intercept σ_f' at one reversal ($N\sigma^b = \sigma_f'$) [BRI 44].

$$\frac{\sigma_a}{\sigma_a'} + \frac{\sigma_m}{\sigma_f'} = 1 \quad [1.69]$$

which results in the following formula:

$$\sigma_a = \sigma_a' \left(1 - \frac{\sigma_m}{\sigma_f'} \right) \quad [1.70]$$

Dowling [DOW 04] considers this method to be appropriate for ductile materials. It seems to be acceptable for aluminum alloys and not as good for steels as the Morrow method using the true stress at fracture.

Walker [WAL 70] gives a relation in which an additional parameter is involved γ :

$$\sigma_a' = \sigma_{\max}^{1-\gamma} \sigma_a^\gamma \quad [1.71]$$

This parameter γ is a fitting constant characteristic of the material. The interest of this parameter lies in the possibility of better representing the experimental results than previous methods.

The value actually observed lies between 0.25 and 0.53 [NIH 86]. Choosing a conventional value equal to 0.5 is often proposed.

If R is the ratio between the minimum stress and the maximum stress of a cycle, this relation can also be expressed from [1.15] as [DOW 04]:

$$\sigma'_a = \sigma_{\max} \left(\frac{1-R}{2} \right)^\gamma \quad [1.72]$$

or

$$\sigma'_a = \sigma_a \left(\frac{2}{1-R} \right)^{1-\gamma} \quad [1.73]$$

K.N. SMITH, P. WATSON and T.H. TOPPER [SMI 70] propose a relation widely used in the uniaxial fatigue calculation (SWT method):

$$\sigma'_a = \sqrt{\sigma_{\max} \sigma_a} = \sqrt{\sigma_a (\sigma_m + \sigma_a)} \quad [1.74]$$

The quadratic equation has only one positive root:

$$\sigma_a = \frac{\sigma_m}{2} \left[\sqrt{\left(\frac{2\sigma'_a}{\sigma_m} \right)^2 + 1} - 1 \right] \quad [1.75]$$

From relation [1.15], this expression can also be written:

$$\sigma'_a = \sigma_{\max} \sqrt{\frac{1-R}{2}} \quad [1.76]$$

or

$$\sigma'_a = \sigma_a \sqrt{\frac{2}{1-R}} \quad [1.77]$$

The SWT model is thus a particular case of the Walker model, for an adjustment coefficient $\gamma = 0.5$, we again find the SWT model.

Bergman and Seeger [BER 79] introduce an additional coefficient in the Smith-Watson-Topper relation, including the sensitivity of the material to the influence of the average stress [NIH 86].

$$\sigma_a = \sqrt{\sigma'_a (k \sigma_m + \sigma'_a)} \quad [1.78]$$

Here, the calculation of σ_a also brings into play the only positive root:

$$\sigma_a = \frac{\sigma_m}{2} \left[\sqrt{\left(\frac{2 \sigma'_a}{\sigma_m} \right)^2 + k} - k \right] \quad [1.79]$$

The SWT relationship corresponds to $k = 1$. The real values observed lie between 0.4 and 0.7 in practice. The value $k = 0.4$ gives the best results with respect to other methods [WEH 91].

All methods should only be used for tensile mean stress values. For cases where the mean stress is small relative to the alternating stress ($R \ll 1$), there is little difference in the methods. As R approaches 1, the models show large differences. There is a lack of experimental data available for this condition, and the yield criterion may set design limits.

Morrow's relationship using the true fracture strength σ_F is distinctly better than the Goodman relationship modified for various metals, but has the disadvantage that values of σ_F are not always available. Morrow with σ'_f works well for steels, but not for aluminum alloys. It gives non-conservative results by predicting lifetimes largely greater than real lifetimes.

The SWT method is a reasonable choice for general use which avoids previous difficulties. It is quite accurate for aluminum alloys, and for steels it is acceptable, although not quite as good as Morrow with σ_F or σ'_f and it tends to be non-conservative for compressive mean stresses. But SWT is consistently better than Morrow with σ_F for the non-ferrous metals [DOW 04].

The Walker approach enables greater precision thanks to the introduction of an adjustable parameter γ . The disadvantage of this model lies in the determination of this coefficient which requires many tests to be carried out.

1.6.2. Statistical representation of Haigh diagram

We saw that in practice, the phenomena of fatigue are represented statistically. The Haigh diagram can take such a form.

For example, if the Gerber relation is chosen, parabolic curves are plotted on the axes σ_a , σ_m to describe the variations of a given stress σ_a corresponding to a given number of cycles to failure with given probability.

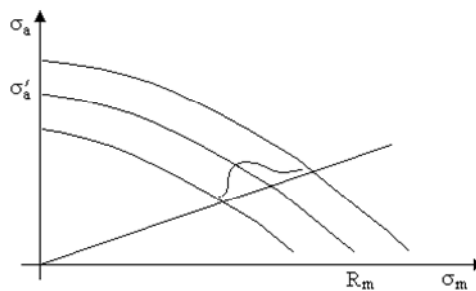


Figure 1.34. Statistical representation of the Haigh diagram

It has been shown that the distribution of the alternating stresses obtained while crossing the arcs of parabola by a straight line emanating from the origin O (slope σ_a/σ_m) is roughly Gaussian [ANG 75].

1.7. Prediction of fatigue life of complex structures

A very difficult problem in the calculation of the fatigue life of a structure is the multiplicity of the sites of initiation of cracks and the mechanisms which determine the life resulting from fatigue of the structure. It could be observed that these sites and mechanisms depend on the environment of service, the amplitude and the nature of the loads.

B.N. Leis [LEI 78] classes fatigue analysis methods into two principal categories:

- indirect approach, in which we try to predict the fatigue life (estimate and accumulation of damage) on the basis of deformation and stress acting far from the potential areas of initiation of the cracks by fatigue, depending on the external displacements and forces (*black box* approach); and

– the direct approach, in which we try to predict the fatigue life on the basis of stress and deformations acting on the potential sites of initiation. These stresses and deformations are local.

The first approach cannot take into account the local inelastic action at the site of initiation of fatigue, whereas the direct approaches can introduce this non-linearity.

The direct approach allows correct predictions of initiation of cracks in a structure provided that the multiplicity of the sites of initiation and mechanisms which control the life in fatigue are correctly taken into account.

1.8. Fatigue in composite materials

An essential difference between metals and composites lies in their respective fatigue behavior. Metals usually break by initiation and propagation of crack in a manner which can be predicted by fracture mechanics. The composites present several modes of degradation such as the delamination, failure of fibers, disturbance of the matrix, presence of vacuums, failure of the matrix and failure of the composite. A structure can present one or several of these modes and it is difficult to say *a priori* which will prevail and produce the failure [SAL 71].

Another difference with metals relates to behavior due to low frequency fatigue. It is often admitted that metals follow, for a low number of cycles, *Coffin-Manson's* law relating the number of cycles to failure N to the strain range. This is of the form:

$$\Delta\varepsilon_p N^\beta = C \quad [1.80]$$

where $\beta \approx 0.5$. The composites are more sensitive to the strain range and more resistant to fatigue when undergoing large numbers of cycles than with a low number of cycles. A structure can break due to the part of the load spectrum relating to small stresses if it is metallic, whereas the same structure in composite would break because of high loads.

The fatigue strength of composite materials is affected by various parameters which can be classified as follows [COP 80]:

– factors specific to the material: low thermal conductivity, leading to an important increase in the temperature if the frequency is too high, defects related on the heterogenous structure of material and its implementation (bubbles, etc.), natural aging related to its conditions of storage, etc.;

– factors related to the geometry of the test bars:

- shape, holes, notches (stress concentration factors), as with metals;
- irregularities of surface being able to modify the thickness of the test bars in a significant way (important in the case of non-uniform stresses (torsion, bending, etc.);

– stress and environment conditions:

- mode of application of the stresses (torsion, etc.),
- frequency,
- mean stress,
- hygrothermic environment, and
- corrosion (surface deterioration of polymer comparable with corrosion).

For example, R. Cope and A. Balme [COP 80] show that a resin polyester-fiberglass composite or laminate obeys a fatigue degradation model because of:

- degradation of the interface fiber-resin;
- degradation by cracking and loss of the resin polyester; and
- progressive damage of the reinforcement.

They use an index of reference for damage evolution depending on the number n of cycles of the ratio G/G_0 (where G is rigidity modulus in torsion after n cycles and G_0 is the same modulus at the test commencement) and observe a threshold n_S . Beyond this threshold, the material starts to adapt in an irreversible way and undergo damage.

The effect of temperature results in a decrease of the threshold n_S for weak deformations and an increase in the number of cycles for failure (for $t > 60^\circ\text{C}$).

The presence of mean stress amplifies the fatigue damage in an important way.

It is often considered that Miner's rule strongly overestimates the fatigue life of the structures in composites [GER 82].